CHAPTER 5
PREPARATION OF Ni LOADING ON NANO-SIZED CeO_2 AND CeO_2-ZrO_2 BY COLLOIDAL EMULSION APHRONS METHOD

5.1 Introduction

One of the most important roles of CeO_2 in these multi-component systems is to provide surface active sites and to act as an oxygen storage/transport medium by shifting between Ce^{3+} and Ce^{4+} under reductive and oxidizing conditions, respectively. These redox properties are strongly enhanced if foreign cations such as Zr, Gd, Pr, and Pb are introduced into the CeO_2 lattice by forming solid solutions. This is the result of enhanced oxygen ion mobility inside the modified fluorite lattice originating from the formation of a defective. Special attention has been focused in recent years on the preparation of ceria structurally doped with ZrO_2. These materials show enhanced thermal, redox, and catalytic properties compared to pure undoped ceria. Their commercial development is being actively pursued [15, 21, 54-57].

One of the promising catalyst systems is metal-CeO_2-ZrO_2, where the metal is nickel, platinum or palladium. The most interesting of metal catalyst is Ni because Ni catalysts have been reported to provide too high endothermic reforming reactivity for in-stack reforming in SOFCs. The rapid endothermic reaction can lead to local temperature gradients especially close to the entrance of the reformer, which consequently cause the possible mechanical failure due to thermally induced stresses [15]. Shan *et al.* [21] had researched on Ni/CeO_2 catalysts. It was found that the highly dispersed NiO showed good redox property with the adsorbed oxygen and oxygen vacancy. In addition, NiO was the active site for methane combustion. Palikanon *et al.* [19] synthesized Ni/CeO_2-ZrO_2 by surfactant-assisted method showed that the great advantage of using Ni on high surface area CeO_2-ZrO_2 based supports were high reforming reactivity and also the high stability due to their excellent resistance toward carbon formation.

In previous chapter nano-sized CeO_2 was successfully prepared by colloidal emulsion aphrons method. The goal of this chapter is to use CeO_2 as a catalyst support material in

methane steam reforming but many researchers showed that only CeO_2-based support give the low reforming reactivity [17, 19, 55-60]. Therefore, in this chapter we improved CeO_2 by adding ZrO_2 for higher thermal stability and selected Ni as an active metal loaded on CeO_2 for the high activity in reforming process with three different procedures. Then, the suitable procedure of preparation which provided the highest hydrogen consumption, the highest surface area, and the highest methane conversion was selected to prepare Ni on CeO_2-ZrO_2.

5.2 Objectives

1) To improve activity toward methane steam reforming of CeO_2 by loaded Ni on CeO_2 with three different procedures of colloidal emulsion aphrons method.

2) To improve thermal stability of CeO_2 catalyst by adding ZrO_2 prepared by colloidal emulsion aphrons method.

3) To investigate the reforming reactivity over all synthesized catalysts.

5.3 Working Scopes

1) Determine the suitable colloidal emulsion aphrons procedure that gives the highest hydrogen consumption, the highest surface area, and the highest methane conversion.

2) At the most suitable preparation procedure, Ni/CeO_2-ZrO_2 was synthesized.

5.4 Experimental

5.4.1 Materials

CeO_2, Ni/CeO_2 and Ni/CeO_2-ZrO_2 were prepared by colloidal emulsion aphrons method with the same starting materials and calcination temperature. All synthesized powder in this part were used ammonium cerium nitrate ($(NH_4)_2Ce(NO_3)_6$) as a cerium source, used zirconyl (IV) nitrate ($ZrO(NO_3)_2$) as a zirconium source, used polyoxyethylene-4-laurylether (PE4LE) as a surfactant, and used nickel nitrate hexahydrate ($Ni(NO_3)_2 \cdot 6H_2O$) as an active metal. The catalyst particles were reduced with 10% H_2/Ar at 900°C for 6 h before use.

5.4.2 Preparation of Ni loading on nano-sized CeO_2 by colloidal emulsion aphrons method

5.4.2.1 Method I

Ni/CeO_2 was prepared by impregnated CeO_2 (from CEAs preparation) into $Ni(NO_3)_2$ solution (10 wt.% Ni). Then, it was stirred at 500 rpm for 2 h. After stirring, the mixed solution was placed into centrifuge tube operated at speed of 12,000 rpm for 15 min to separate the precipitate from the solution. The precipitate was washed with ethanol followed by centrifugation again in order to completely remove both residual external phase and organic membrane phase for 2 times. The precipitate was dried at 100°C for 1 h and finally was calcined at 500°C for 3 h.

5.4.2.2 Method II

Ni/CeO_2 was prepared by impregnated CeO_2 (from CEAs preparation) into colloidal emulsion aphrons of nickel solution under vigorously stirred for 2 h. After stirring, the cleaning procedure was the same as described in Method I.

5.4.2.3 Method III

Ni/CeO_2 was prepared by added an external water phase containing cerium solution and nickel solution into CEAs, the mixed solution was stirring at vigorously. After stirring, the cleaning procedure was the same as described in Method I.

5.4.3 Preparation of nano-sized CeO_2-ZrO_2 and Ni/CeO_2-ZrO_2 by colloidal emulsion aphrons method

CeO_2-ZrO_2 was prepared by colloidal emulsion aphrons method. An internal phase of mixed W/O emulsion (cerium source emulsion and zirconium source emulsion, with Ce/Zr molar ratio of 3/1) was added to the colloidal gas aphrons (CGAs) under stirring at vigorously. The colloidal gas aphrons was prepared by adding Tween80 (6 ml) into deionized water (60 ml). The solution was mixed with a homogenizer at the rotation of 12,000 rpm for 2 min. After stirring for 1 h, the colloidal emulsion aphrons (CEAs) were obtained. Then, an external water phase containing $N_2H_4 \cdot H_2O$ was added into CEAs. The mixed solution was vigorously stirred for 30 min. After stirring, the mixed solution became dark brown. Then, it was placed into centrifuge tube operated at speed of 12,000 rpm for 15 min to separate the precipitate from the solution. The precipitate

was washed with ethanol followed by centrifugation for 2 times in order to completely remove both residual external phase and organic membrane phase. The precipitate was dried at 100°C for 1 h and calcined at 900°C for 3 h. CeO_2-ZrO_2 powders was obtained.

Ni/CeO_2-ZrO_2 was prepared by impregnation of CeO_2-ZrO_2 powder into colloidal emulsion aphrons of Ni under vigorously stirred for 2 hr. After stirring, the mixed solution was placed into centrifuge tube and centrifugation at a speed of 12,000 rpm for 15 min to separate the precipitate from the solution. The precipitate was washed with ethanol followed by centrifugation in order to completely remove both residual external phase and organic membrane phase for 2 times. The precipitate was dried at 100°C for 1 h and finally was calcined at 900°C for 3 h. Ni/CeO_2-ZrO_2 powder was finally obtained.

5.4.4 Characterization Techniques

The crystalline structure of the prepared Ni/CeO_2 was determined by X-ray diffractometer (XRD, Bruker: D8-Discover) using CuKα radiation (λ = 1.542 Å) operating at 40 kV and 40 mA, scaned rate at 0.02 degree/step over the angular ranges of 2θ = 10-100°. The Brunaur-Emmett-Teller (BET) surface area and pore size distributions of the sample were measured from the nitrogen adsorption/desorption at 77 K using a Quantachrom Autosorb-1 surface area and pore size analyzer. The average particle size was observed by transmission electron microscope (TEM, Jeol Model JEM-2100). The oxygen storage capacities and the degree of redox properties for Ni/CeO_2 were investigated by using temperature programmed reduction (TPR) due to the amount of hydrogen uptake relates to the amount of free oxygen on the surface of the particles. TPR was done by introducing 4.95% H_2 in nitrogen while heating the system up to 900°C. The weight contents of Ni and molar ratio of Ce/Zr were determined by X-ray fluorescence (XRF) analysis.

5.4.5 Methane steam reforming [17]

An experimental reactor system consists of three main sections: feed, reaction and analysis sections. The feed gases including the component of interest (CH_4, H_2O, H_2 or O_2) were introduced in the reactor section, where an 8 mm internal diameter and 40 cm length quartz reactor was mounted vertically inside a furnace. The synthesized powder was loaded in the quartz reactor, which was packed with a small amount of quartz wool

to prevent the catalyst from moving. A Type-K thermocouple was placed into the annular space between the reactor and the furnace. This thermocouple was mounted on the reactor in close contact with the catalyst bed to minimize the temperature difference between the catalyst bed and the thermocouple. After the reactions, the exit gas mixture was transferred via trace-heated lines to the analysis section, which consists of a Porapak Q column Shimadzu 14B gas chromatography and a mass spectrometer. The gas chromatography was applied in order to investigate the steady state condition of the experiments, whereas the mass spectrometer was used for the transient carbon formation.

5.5 Results and Discussion

5.5.1 Characterization of Ni/CeO_2 prepared by three different procedures

Figure 5.1 shows the XRD patterns of the synthesized particles obtained from different method of preparation. All the reflection in Figure 5.1 showed the small peak of NiO because the product was loaded with Ni 10%wt. Therefore, to confirm the Ni content in synthesized powder, the powders were determined by XRF, presented in Table 5.1.

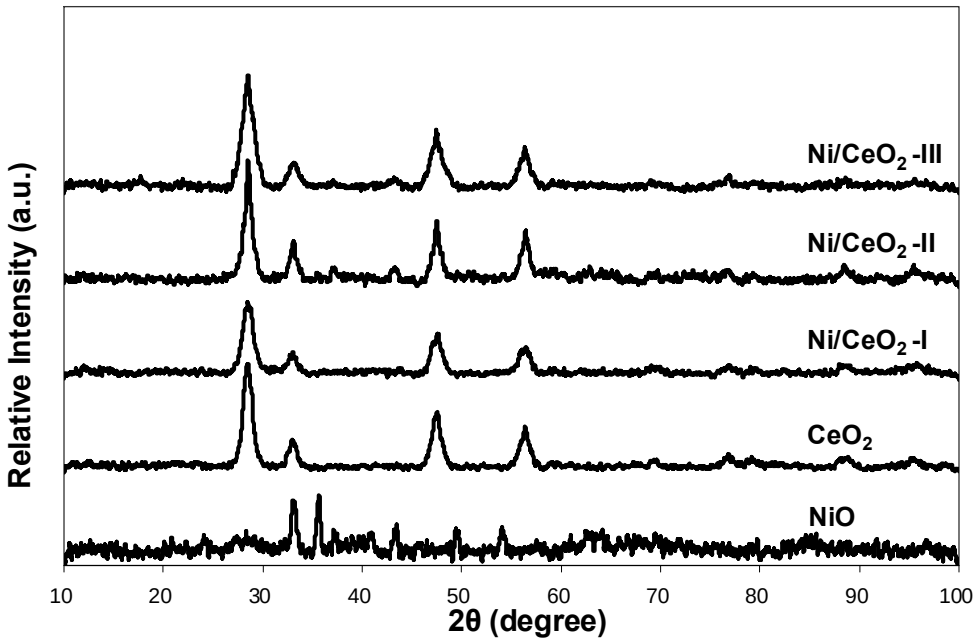

Figure 5.1 XRD patterns of synthesized particle prepared by different methods.

Table 5.1 Surface area, porosity, average particle size, and percent yield of CeO_2 and Ni/CeO_2 prepared by different methods of CEAs.

Catalyst	% Ni loading	Surface area (m^2/g)	Pore volume (cm^3/g)	Pore size (Å)	Average particle size (nm)
CeO_2	0.0	145.73	0.2169	59.30	4.7 ± 0.1
Ni/CeO_2-I	10.0	11.86	0.1183	39.89	6.4 ± 0.2
Ni/CeO_2-II	9.1	89.64	0.1175	52.42	9.3 ± 0.2
Ni/CeO_2-III	9.9	117.40	0.1950	66.42	5.1 ± 0.3

The surface area of Ni/CeO_2 prepared by Method I, Method II, and Method III with the same starting materials were 11.86, 89.64, and 117.40 m^2/g, respectively. The result showed that the surface area of CeO_2 after loading with Ni decreased. The surface area of Ni/CeO_2 obtained from Method III was the highest. It showed the smallest average particle size. The porosity analysis were summarize in Table 5.1

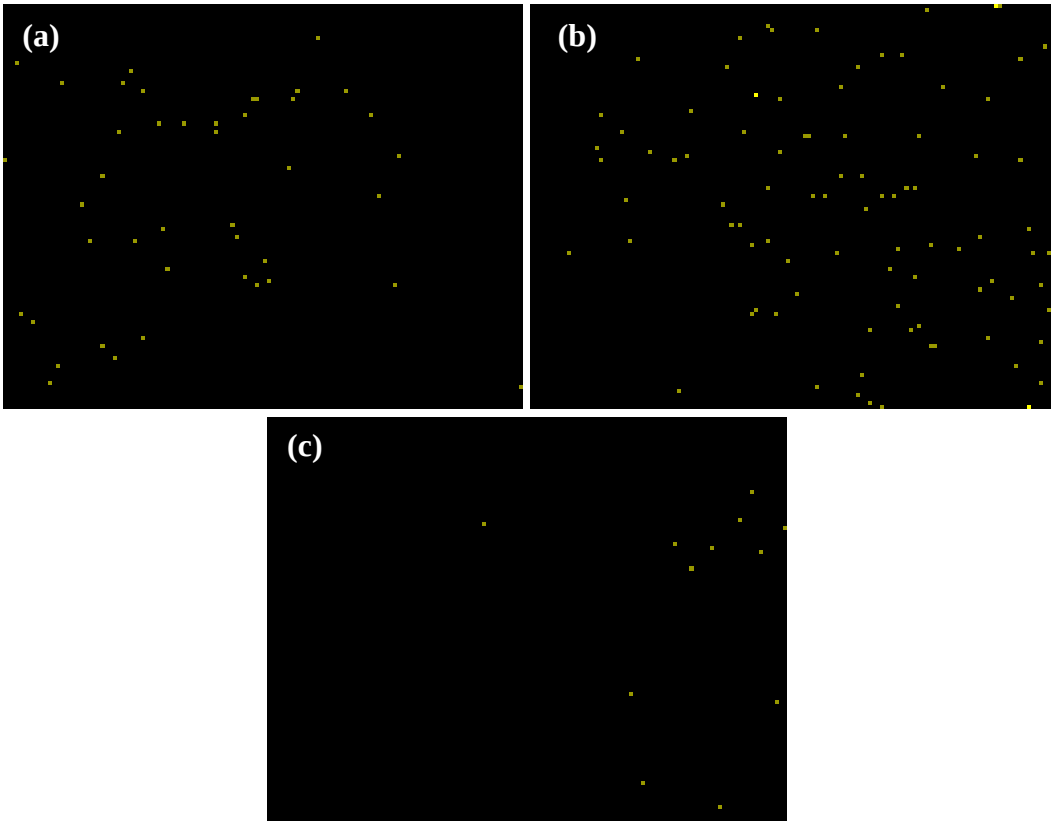

Figure 5.2 EDX mapping images of Ni dispersed on CeO_2 support prepared by different methods (a) Method I, (b) Method II, and (c) Method III.

Figure 5.2 shows Ni dispersion on CeO_2 support prepared by different methods. The results showed that Ni/CeO_2 prepared by Method II showed good Ni dispersion on CeO_2 compared with Method I and Method III. Ni dispersion in Method I was better than Method III. The preparation in Method I and Method II used CeO_2 powder while in Method III used cerium solution as a starting support material. Therefore, in Method III Ni might be dispersed in the pore of CeO_2 hence Ni at the catalyst surface was less than that of Method I and II. In comparison of Method I and II, in Method I CeO_2 powder was impregnated into nickel solution but Method II CeO_2 was impregnated into colloidal emulsion aphrons of nickel solution. Considering to the structure of CEAs, the dispersion of Ni in CEAs should be better than nickel solution resulting in well deposit of Ni on CeO_2 surface.

As described earlier, the oxygen storage capacities and the degree of redox properties for catalysts were investigated by using temperature programmed reduction (TPR) due to the amount of hydrogen uptake related to the amount of free oxygen on the surface of the particles. TPR was done by introducing 4.95%H_2 in nitrogen while heating the system up to 900°C. The result of hydrogen uptakes from the mass spectrometer signal were detected from varieties of Ni/CeO_2 including CeO_2 as shown in Figure 5.3.

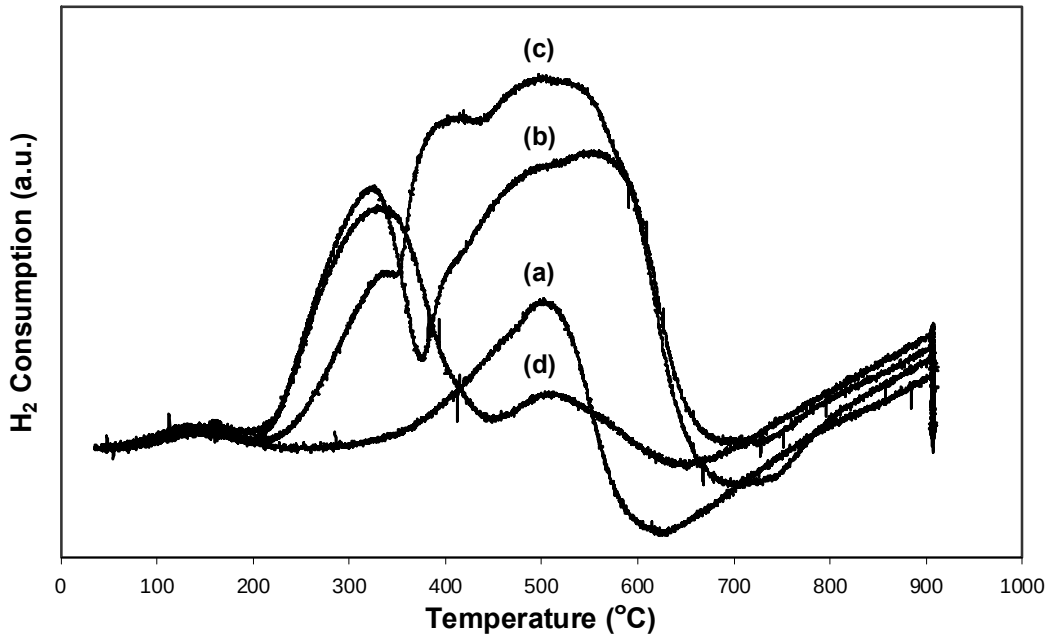

Figure 5.3 Temperature programmed reduction (TPR) of CeO_2 and Ni/CeO_2 prepared by different methods (a) CeO_2, (b) Ni/CeO_2-I, (c) Ni/CeO_2-II, and (d) Ni/CeO_2-III.

As presented in Figure 5.3, the amount of hydrogen uptakes of Ni/CeO_2 sample prepared by Method II was significant higher than the other samples whereas pure CeO_2 had the lowest amount of hydrogen uptake. The amount of hydrogen uptakes of Ni/CeO_2 sample prepared by Method III was higher than Method I. The result indicated that, according to these experimental conditions, the occurrence of redox properties for samples which were loaded Ni had much more activity than pure CeO_2.

5.5.2 Methane steam reforming over Ni/CeO_2 prepared by three different methods

The synthesized CeO_2 and Ni/CeO_2 were studied in the methane steam reforming at 900ºC. The inlet components were $CH_4/H_2O/H_2$ in helium with the inlet ratio of 1.0/3.0/0.2. The main products from the reactor over CeO_2 were H_2 and CO with some CO_2, indicating a contribution from the water-gas shift, and the reverse methanation at this high-temperature.

Table 5.2 The result of all catalysts after methane steam reforming process.

Catalyst	Methane conversion (%)						Carbon formation (mmol/g)
	1h	2h	3h	4h	5h	6h	
CeO_2	29.8	26.4	23.9	18.9	16.4	15.6	0.52
Ni/CeO_2-I	58.4	53.9	46.2	44.1	43	43.8	2.79
Ni/CeO_2-II	71.0	68.9	68.4	67.5	67.3	67.2	1.92
Ni/CeO_2-III	51.9	49.2	48.6	47.1	47.9	47.5	1.48

The conversions of CH_4 with time for all catalysts are given in Table 5.2. It was found that the conversion of CH_4 of CeO_2, Ni/CeO_2 (Method I), Ni/CeO_2 (Method II), and Ni/CeO_2 (Method IIII) were 15.6, 43.8, 67.2, and 47.5%, respectively. The quantities of carbon deposited on the CeO_2, Ni/CeO_2 (Method I), Ni/CeO_2 (Method II), and Ni/CeO_2 (Method IIII) surface were 0.52, 2.79, 1.92, and 1.48 mmol/g, respectively. The result shows that the methane conversion of Ni/CeO_2 prepared by Method II was the highest.

As the surface area of Ni/CeO_2 obtained from Method III were the highest therefore the methane reforming reactivity should be the highest too. However, the result showed that

the methane conversion of Ni/CeO_2 prepared by Method II was the highest at 67.2%, whereas the methane conversion of Method I and III were 43.8 and 47.5%, respectively. The result could be explained by the characterization of EDX mapping and TPR as shown in Figure 5.2 and Figure 5.3. From EDX mapping images indicated that Ni/CeO_2 Method II showed good Ni dispersion on CeO_2 compared with Method I and III. Ni dispersion in Method I was better than Method III, which meant the reforming reactivity of Ni/CeO_2 prepared by Method I should be more than Ni/CeO_2 prepared by Method III. On the other hand, Ni/CeO_2 prepared by Method III show the higher methane conversion than Method I. Although the Ni dispersion in Method III is not better than Method I but Ni/CeO_2 prepared by Method III have high surface area and Ni might be in the pore of CeO_2. From the TPR analysis, can confirm the reason of reforming reactivity results.

The all characterization and the methane steam reforming results of Ni/CeO_2 indicated that Ni/CeO_2 obtained from Method II (impregnated CeO_2 into colloidal emulsion aphrons of nickel solution) showed the highest amount of hydrogen uptakes and the highest methane conversion. Therefore, this method was a suitable method for the catalyst preparation in future work.

5.5.3 Surface area of the support materials

The surface area of CeO_2 and CeO_2-ZrO_2 were determined by BET as shown in Table 5.3. After drying, surface areas of 201.40, and 235.78 m^2/g were observed for CeO_2 and CeO_2-ZrO_2, respectively. The surface area decreased at high calcination temperature. According to the experiment, adding ZrO_2 to CeO_2 provided higher surface area than those of pure CeO_2, which indicated the increasing of the thermal stability. The result in Table 5.3 shows that after drying surface areas of 108.8 m^2/g were observed for ZrO_2. Then, after calcination at 600 ºC the surface area decreased to 92.1m^2/g. As a result, the reduction of ZrO_2 surface area was 15.3%, which was lower than pure CeO_2 (32.2%). Therefore, ZrO_2 had higher thermal resistance than CeO_2. It should be noted that the introduction of ZrO_2 could stabilize the surface area of CeO_2, which was in a good agreement with the results obtained on catalysts prepared by conventional routes [19, 62]. This was probably due to the inhibition of the sintering process induced by the dopant ion [62]. Moreover, Ozawa *et al.* [60] reported that the addition of ZrO_2 to CeO_2

improved the activity of CeO_2, the oxygen storage capacity, redox property, and enhanced the removal activity for CO, NO_x and hydrocarbons under dynamic air-fuel ratio condition.

As presented in Table 5.3, the results show that the surface area of CeO_2-ZrO_2 prepared by CEAs method was the highest, which meant the CEAs method was the suitable method for catalyst preparation.

Table 5.3 Surface area of the catalyst supports prepared by different methods before and after calcination [13, 19, 54, 59, 63]**.**

Catalyst	Preparation method	Surface area (m^2/g)		
		After drying at 100°C	After calcination at 600°C	After calcination at 900°C
CeO_2	CEAs	201.4	136.3	47.6
CeO_2	Surfactant-assisted	105.0	21.0	24.0
CeO_2	Precipitation	55.0	48.0	8.5
CeO_2	NanoArc	82.0	56.0	35.0
CeO_2	Mechanical milling	-	5-18 (700°C)	-
ZrO_2	CEAs	108.8	92.1	-
CeO_2-ZrO_2	CEAs	235.8	163.4	60.5
CeO_2-ZrO_2	Surfactant-assisted	115.0	-	40.0
CeO_2-ZrO_2	Precipitation	70.0	-	19.0
CeO_2-ZrO_2	Mechanical milling	-	5-18 (700°C)	-
CeO_2-ZrO_2	Sol-gel	-	60-90 (523°C)	-

5.5.4 Characterization of all catalysts

5.5.4.1 X-ray diffraction

Figure 5.4 shows the XRD patterns of all catalysts prepared by colloidal emulsion aphrons methods. The peak of NiO was not presented in all the reflection in Figure 5.4.

As the synthesized powder was load with Ni 5%wt and the NiO highly dispersed as smaller crystallites resulting in they were not detected by XRD techniques [8]. Therefore, in order to confirm Ni content and molar ratio of Ce/Zr (3/1) in the synthesized powder were examined by XRF, as presented in Table 5.4.

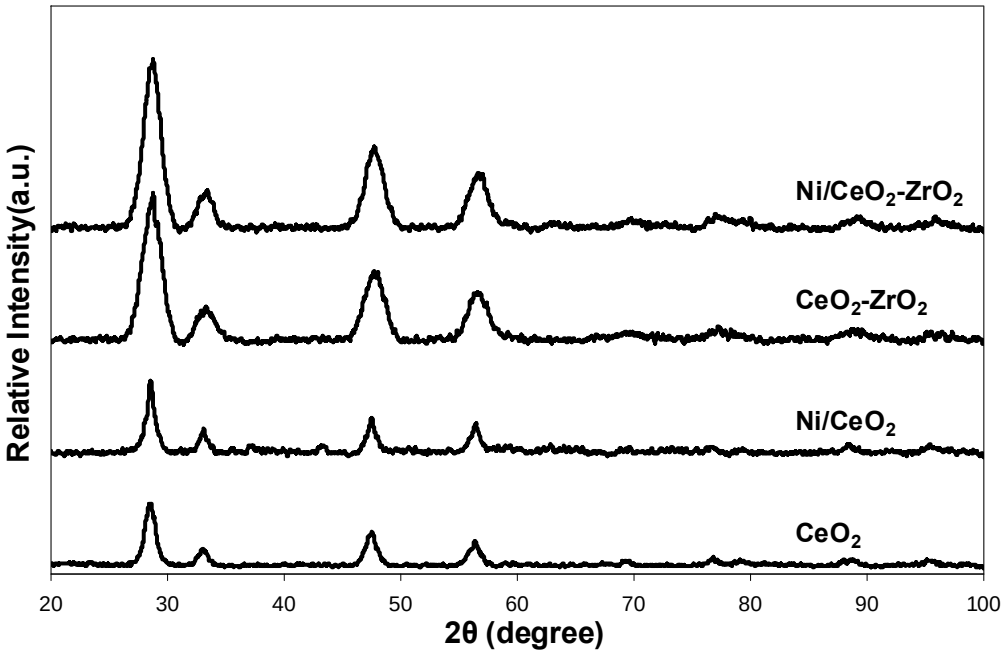

Figure 5.4 XRD patterns of all catalysts prepared by CEAs method.

5.5.4.2 Specific surface area, pore size, and pore volume

Improvements of stability and activity toward methane steam reforming were achieved for Ni on CeO_2 and CeO_2-ZrO_2 based supports. The higher stabilities showed are caused by the lower reduction of surface area compared to Ni on CeO_2 and CeO_2-ZrO_2 based supports.

The BET measurement, as presented in Table 5.4, suggested that the deactivations of Ni/CeO_2 and Ni/CeO_2-ZrO_2 were mainly due to the reduction of surface area. However, the reduction percentage of Ni/CeO_2 and Ni/CeO_2-ZrO_2 prepared by CEAs method were the lowest, indicating the high stability of CeO_2 and CeO_2-ZrO_2 toward the thermal sintering.

Table 5.4 Surface area of all catalysts prepared by different methods before and after reaction.

Catalyst	Ni-load* (wt. %)	Surface area (m^2/g)		
		Before reaction	After reaction	Surface area reduced (%)
Ni/CeO_2[a]	4.9	44.3	43.0	2.9
Ni/CeO_2[b]	-	24.0	22.0	8.3
Ni/CeO_2[c]	4.8	8.5	6.2	27.0
Ni/CeO_2-ZrO_2[a]	4.8	59.2	58.1	1.8
Ni/CeO_2-ZrO_2[b]	-	40.0	39.0	2.5
Ni/CeO_2-ZrO_2[c]	4.8	19.0	18.0	4.5

* Measured from X-ray fluorescence analysis.

[a] Prepared by colloidal emulsion aphrons method.

[b] Prepared by the surfactant-assisted approach [19].

[c] Prepared by the precipitation method [17, 19].

Most catalysts are inherently porous. Many techniques have been developing to characterize the porous structure of solids. Among them the nitrogen adsorption technique is the most popular one that can obtain the data on the BET surface area, total pore volume, and pore size distribution. The adsorption/desorption isotherms are grouped into six types followed the International Union of Pure and Applied Chemistry (IUPAC) as discussed in Chapter 3. The N_2 adsorption/desorption isotherms for all catalysts prepared by CEAs method are shown in Figure 5.5, 5.6, 5.7, and 5.8. The isotherms were similar to type IV isotherm with a hysteresis loop for all catalysts. The hysteresis loops were associated with capillary condensation taking place in mesopores. According to IUPAC classification of hysteresis loops (Figure 3.9), the hysteresis loops of CeO_2, CeO_2-ZrO_2, and Ni/CeO_2-ZrO_2 were similar to type H3 shape corresponding to the adsorption in slit-shaped pored [39] while the hysteresis loops of Ni/CeO_2 similar to type H1 shape corresponding to the adsorption in regular pored and narrow size distribution.

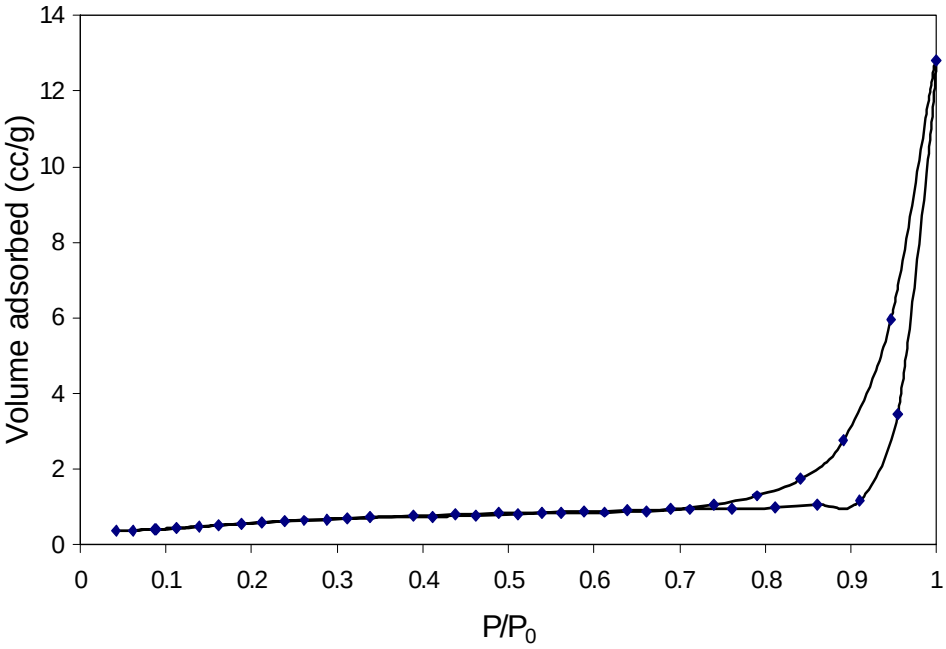

Figure 5.5 N_2 adsorption/desorption isotherm for CeO_2 prepared by CEAs.

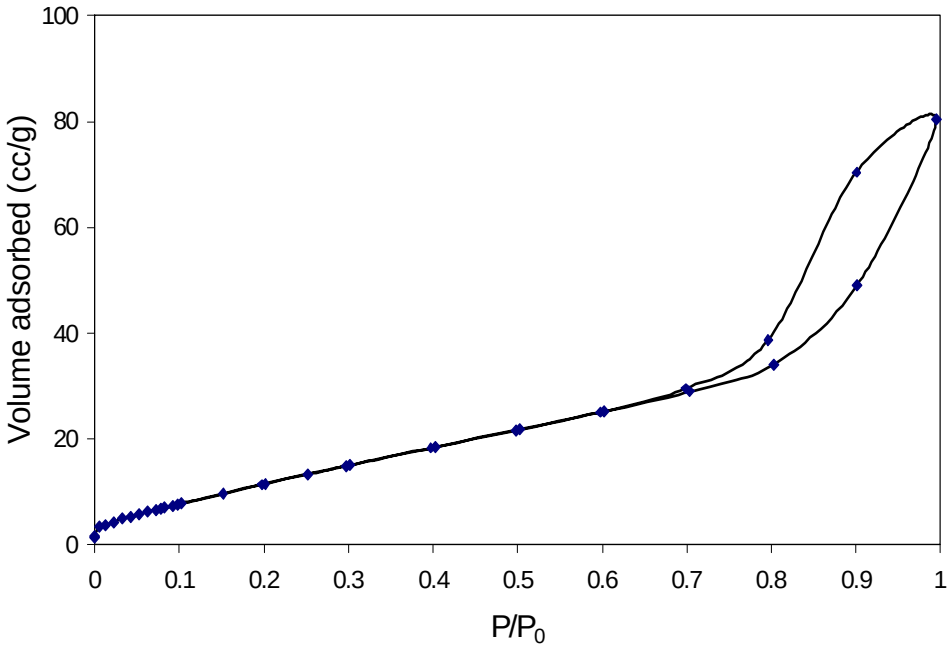

Figure 5.6 N_2 adsorption/desorption isotherm for CeO_2-ZrO_2 prepared by CEAs.

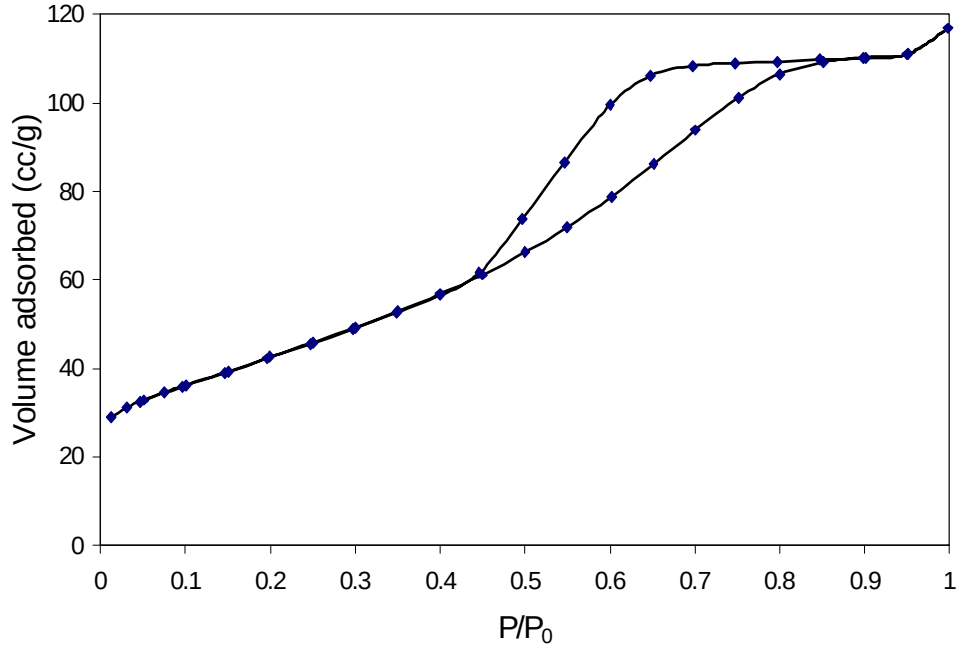

Figure 5.7 N_2 adsorption/desorption isotherm for Ni/CeO_2 prepared by CEAs.

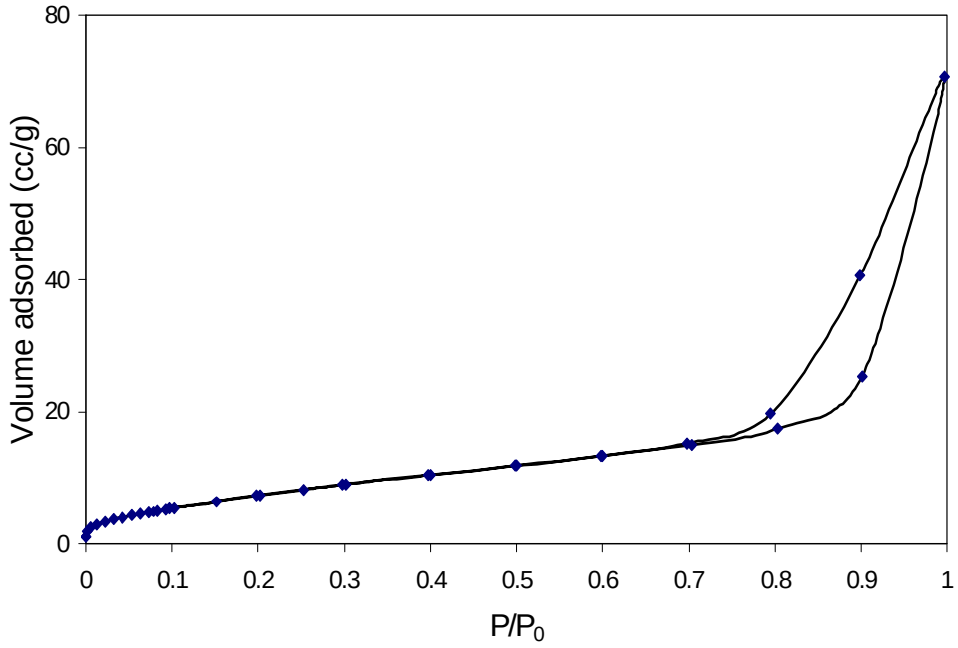

Figure 5.8 N_2 adsorption/desorption isotherm for Ni/CeO_2-ZrO_2 prepared by CEAs.

Table 5.5 summarizes the results of specific surface area, pore volume, and average pore diameter of all catalysts and pore size distribution of all catalysts are shown in Figure 5.9, 5.10, 5.11, and 5.12. It was observed that specific surface areas (S_{BET}) were relatively high for mixed oxide of ceria and zirconia. The results of total pore volume (V_T) showed the similar trend as of S_{BET}.

Table 5.5 Total pore volume, surface area and average pore diameter of all catalysts prepared by CEAs method.

Sample	Pore volume (cm^3/g)			Surface area (m^2/g)			D (Å)
	V_T	V_{me}	V_{mi}	S_{BET}	S_{me}	S_{mi}	
CeO_2	0.0470	0.0470	0.0000	47.6	47.6	0.0	50.7
CeO_2-ZrO_2	0.1747	0.1711	0.0036	60.5	50.5	10.0	50.8
Ni/CeO_2	0.1796	0.1796	0.0000	44.3	44.3	0.0	47.1
Ni/CeO_2-ZrO_2	0.1737	0.1677	0.0060	59.2	43.8	15.4	48.4

V_T: Total pore volume, V_{me}: Mesopore volume, V_{mi}: Micropore volume,
S_{BET}: BET surface area, S_{me}: Mesopore surface area, S_{mi}: Micropore surface area,
D: Average pore diameter.

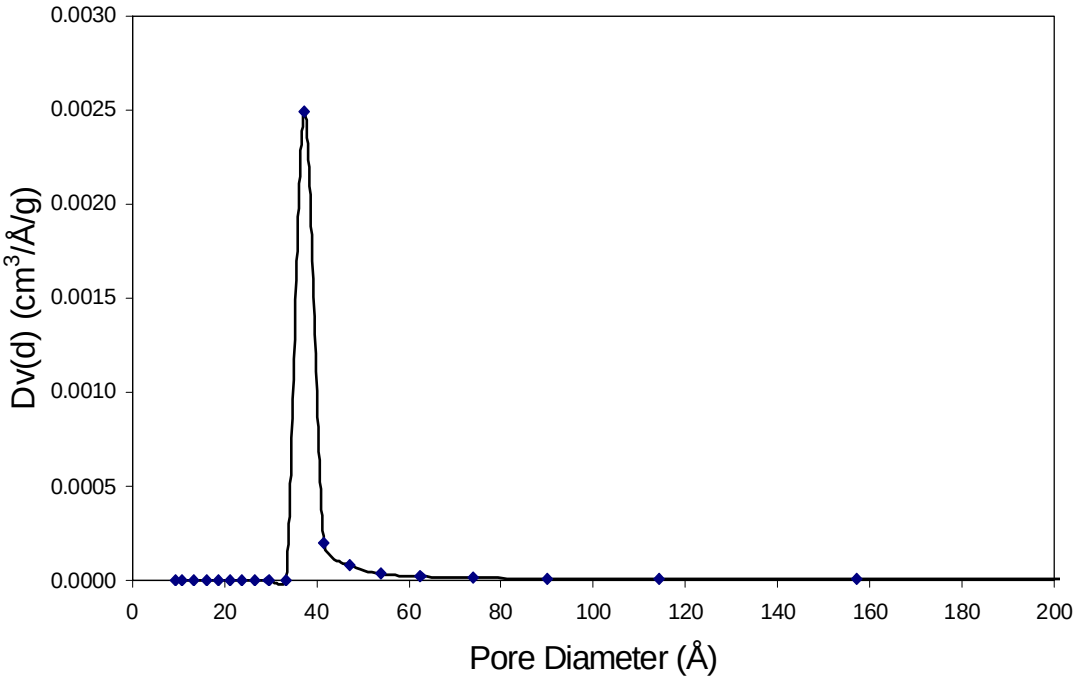

Figure 5.9 Pore size distribution of CeO_2 prepared by CEAs.

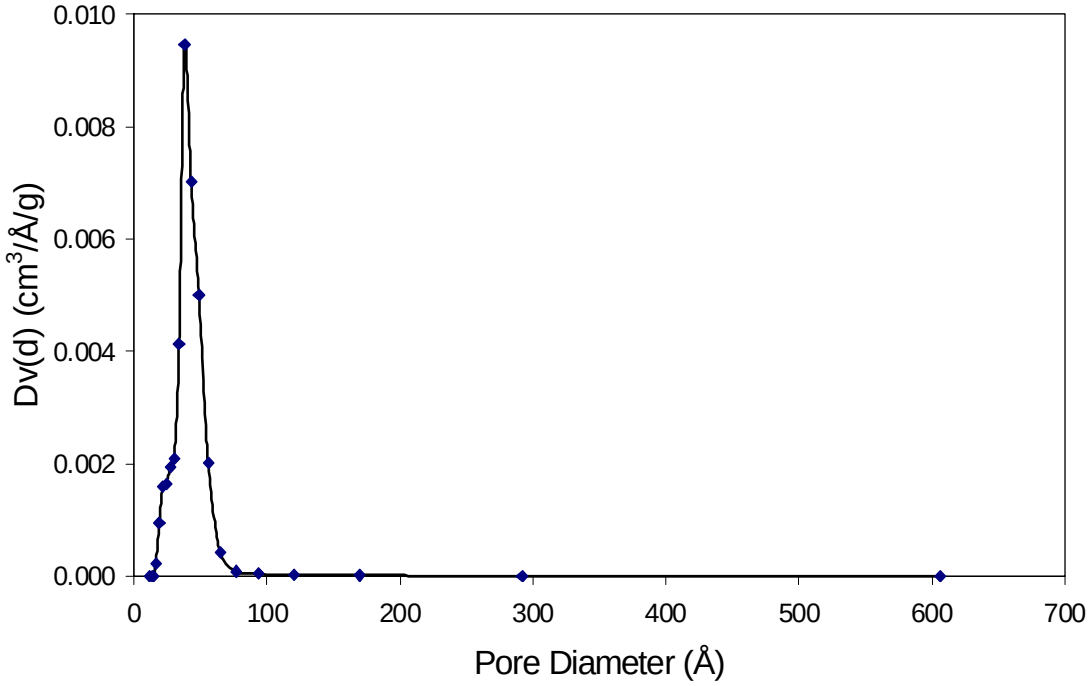

Figure 5.10 Pore size distribution of CeO_2-ZrO_2 prepared by CEAs.

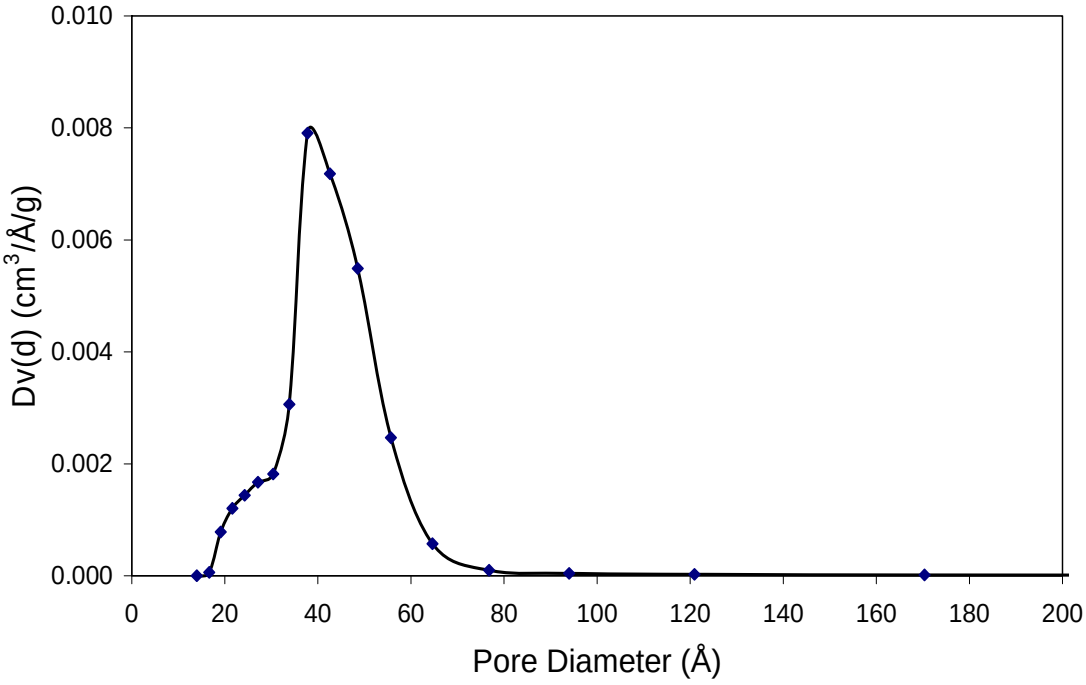

Figure 5.11 Pore size distribution of Ni/CeO_2 prepared by CEAs.

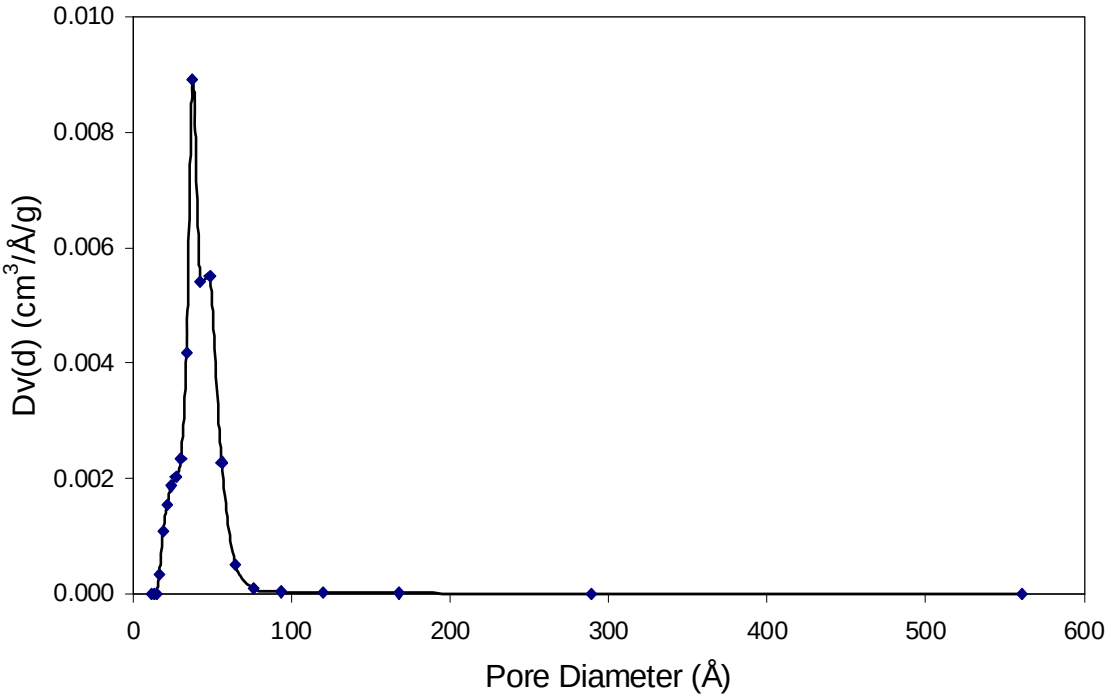

Figure 5.12 Pore size distribution of Ni/CeO_2-ZrO_2 prepared by CEAs.

5.5.4.3 Temperature programmed reduction (TPR)

The oxygen storage capacities and the degree of redox properties for catalysts were investigated by using temperature programmed reduction (TPR) due to the amount of hydrogen uptake relates to the amount of free oxygen on the surface of the particles. TPR was done by introducing 4.95%H_2 in nitrogen while heating the system up to 900°C and the result of hydrogen uptakes from the mass spectrometer signal as shown in Figure 5.13.

As presented in Figure 5.13, the amount of hydrogen uptakes of Ni/CeO_2-ZrO_2 sample was significant the highest. The pure CeO_2 had the lowest amount of hydrogen uptake, whereas no hydrogen uptakes were observed from pure ZrO_2 [19]. The result indicated that, according to these experimental conditions, the occurrence of redox properties for samples which added ZrO_2 had much more activity than the pure CeO_2 and Ni/CeO_2. This is should be caused by the relation between the surface area of the support material and the redox properties. As described earlier, adding ZrO_2 provided higher surface area than pure CeO_2 and led to the high hydrogen uptake during the TPR analysis, which means the increasing of oxygen storage capacity. It should be noted that although pure

ZrO_2 has lowest surface area reduction but the hydrogen uptake during the TPR is zero, which is due to the zero oxygen storage capacity of ZrO_2. This high oxygen storage capacity was associated with enhanced reducibility of cerium (IV) in CeO_2–ZrO_2, which is a consequence of the high O^{2-} mobility inside the fluorite lattice. One possible reason for the increasing mobility might be related to the lattice strain, which is generated by the introduction of a smaller isovalent Zr cation into the CeO_2 lattice (Zr^{4+} has a crystal ionic radius of 0.84 Å, which is smaller than 0.97 Å for Ce^{4+} in the same co-ordination environment). Due to the high thermal stability of this material, CeO_2–ZrO_2 would be a good candidate to be used as the catalyst support for high temperature steam reforming reactions.

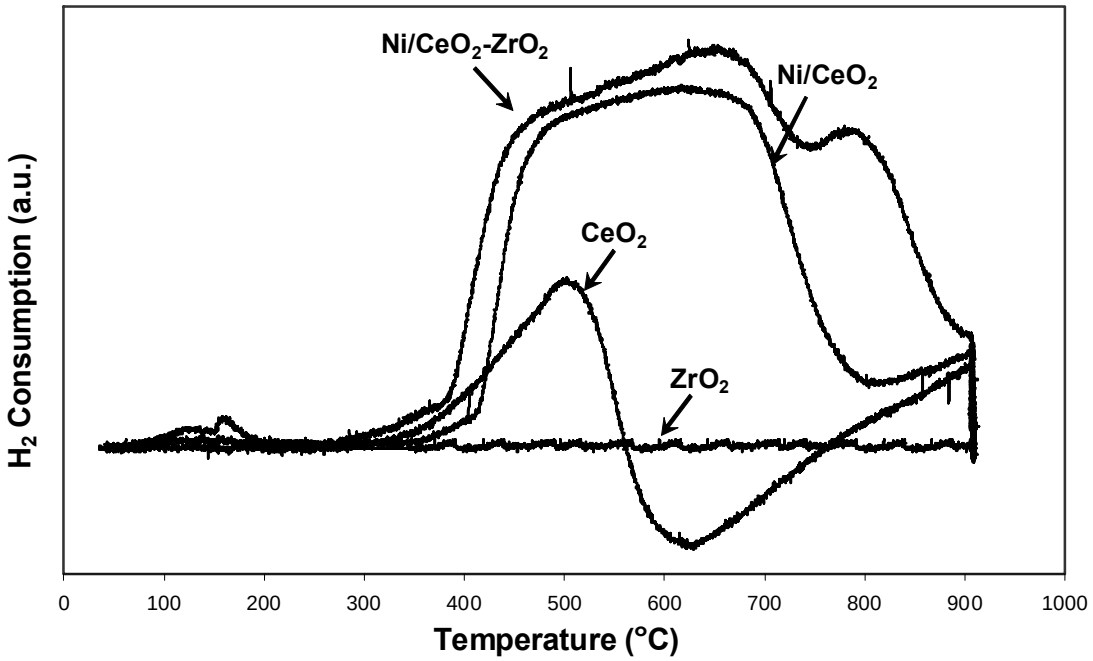

Figure 5.13 Temperature programmed reduction (TPR) of all catalysts.

5.5.4.4 Transmission electron microscope

Figure 5.14 shows the TEM micrographs of all catalysts prepared by CEAs method. The average particle size of Ni/CeO_2, CeO_2-ZrO_2, and Ni/ CeO_2-ZrO_2 were 5.0 ± 0.1, 3.7 ± 0.6, 3.7 ± 0.6 nm, respectively.

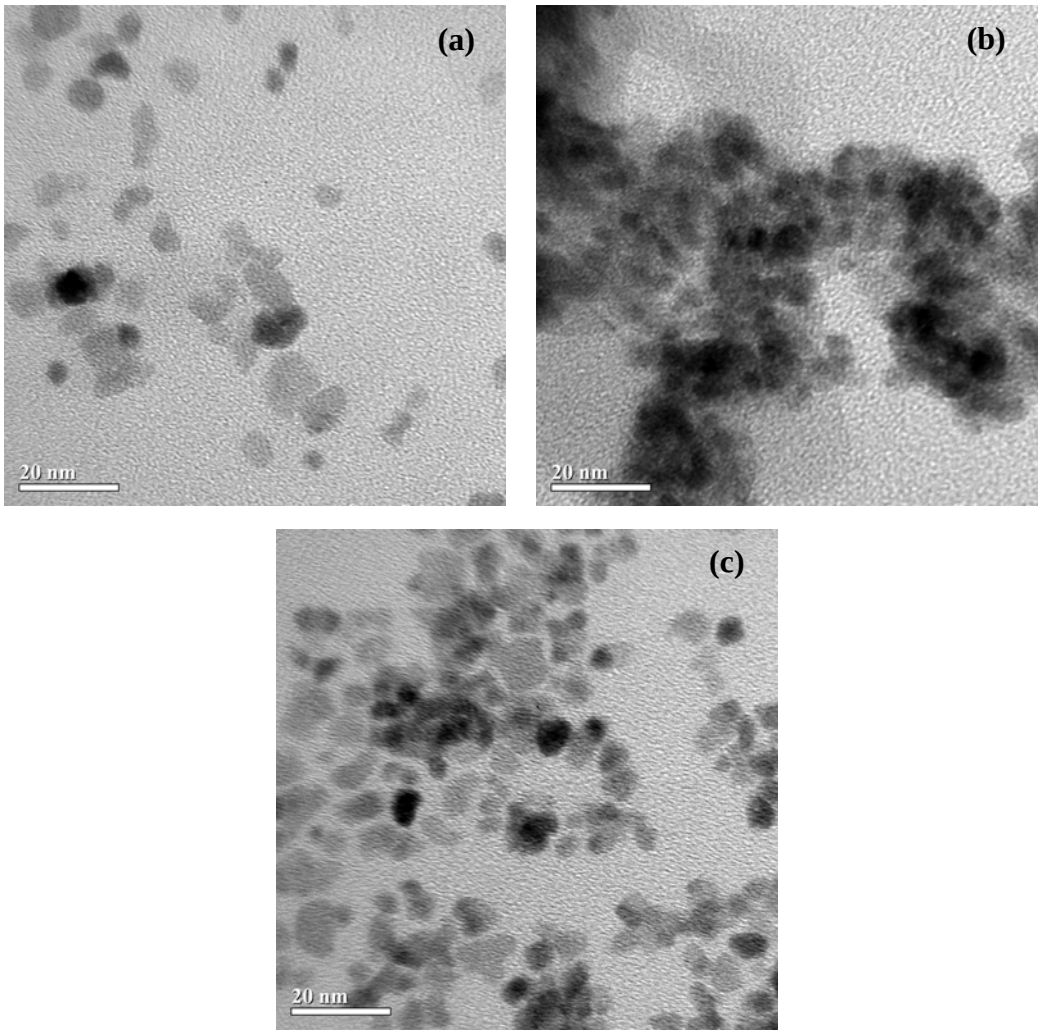

Figure 5.14 TEM micrograph of catalysts before reaction (a) Ni/CeO_2, (b) CeO_2-ZrO_2, and (c) Ni/CeO_2-ZrO_2.

5.5.5 Stability and activity of all catalysts toward methane steam reforming

The synthesized catalysts were tested in the methane steam reforming at 900ºC. At steady state, the conversion of CH_4, H_2 yield, H_2/CO ratio, and the quantities of carbon deposited on catalyst are shown in Table 5.6. In the table, it was found that the CH_4 conversion of CeO_2, CeO_2-ZrO_2, Ni/CeO_2, and Ni/CeO_2-ZrO_2 were 18.9, 24.7, 71.3, and 81.5%, respectively. The quantities of carbon deposited on the CeO_2, CeO_2-ZrO_2, Ni/CeO_2, and Ni/CeO_2-ZrO_2 surface were 0, 0.12, 1.04, and 1.15 mmol/g, respectively.

Table 5.6 The results after methane steam reforming at 900°C.

Catalyst	CH_4 conversion (%)	H_2 yield (%)	H_2/CO ratio	Carbon formation (mmol/g)
CeO_2-ME	7.4	51.3	4.11	0.03
CeO_2-ELM	7.9	54.7	4.23	0.05
CeO_2-CEAs	18.9	71.5	4.05	~0
CeO_2-ZrO_2	24.7	70.1	4.08	0.12
Ni/CeO_2[a]	71.3	77.4	4.14	0.14
Ni/CeO_2[b]	67.0	-	-	0.90
Ni/CeO_2[c]	31.0	-	-	1.25
Ni/CeO_2[d]	27.0	-	-	-
Ni/CeO_2-ZrO_2[a]	81.5	87.4	4.13	0.08
Ni/CeO_2-ZrO_2[b]	69.0	-	-	1.04
Ni/CeO_2-ZrO_2[c]	47.0	-	-	1.29
Ni/CeO_2-ZrO_2[e]	58.1	-	6.80	-

[a] Prepared by colloidal emulsion aphrons method.

[b] Prepared by the surfactant-assisted approach [19].

[c] Prepared by the precipitation method [17, 19].

[d] Prepared by the combustion synthesis [64].

[e] Prepared by the sol-gel method [15].

Methane steam reforming mechanism over conventional Ni catalyst proposed by Dicks *et al.* [46], methane will only adsorb on the active surface site of Ni (*) and forms CH_x-*n. Simultaneously, the adsorption of inlet steam also takes place on the surface site of Ni catalyst forming O-*. These element, O-* and CH_x-*n, eventually reacts each other producing CO and H_2, and also recovers the active surface site of Ni (*) as illustrated below.

$$CH_4 + n* \rightarrow CH_x\text{-}*n + (4\text{-}x)/2H_2 \quad (5.1)$$

$$H_2O + * \leftrightarrow O\text{-}* + H_2 \quad (5.2)$$

$$CH_x\text{-}*n + O\text{-}* \rightarrow CO + x/2H_2 + (n+1)* \quad (5.3)$$

For the steam reforming of methane over Ni/Ce–ZrO_2, in addition to the reactions on Ni surface, the redox reaction between inlet CH_4 and the lattice oxygen (O_x) on CeO_2–ZrO_2 surface also takes place, producing H_2 and CO. Moreover, the reduced CeO_2–ZrO_2 can react with inlet H_2O to produce more H_2 and to recover O_x [17]. The proposed mechanism for these redox reactions, involving the reactions between methane or an intermediate surface hydrocarbon species with the lattice oxygen (O_x) on CeO_2–ZrO_2 surface and the recovery of O_x by steam, is presented schematically below (as discussed in Chapter 3) :

$$CH_4 + 2S \leftrightarrow CH_3\text{-}S + H\text{-}S \quad (3.14)$$
$$CH_3\text{-}S + S \leftrightarrow CH_2\text{-}S + H\text{-}S \quad (3.15)$$
$$CH_2\text{-}S + S \leftrightarrow CH\text{-}S + H\text{-}S \quad (3.16)$$
$$CH\text{-}S + S \leftrightarrow C\text{-}S + H\text{-}S \quad (3.17)$$
$$C\text{-}S + O_x \leftrightarrow CO + O_{x-1} + S \quad (3.18)$$
$$CO + O_x \leftrightarrow CO_2 + O_{x-1} \quad (3.19)$$
$$2H\text{-}S \leftrightarrow H_2 + 2S \quad (3.20)$$
$$H_2O + O_{x-1} \leftrightarrow O_x + H_2 \quad (3.21)$$

The surface site (S) can be either a unique site, or it can also be considered to be the same site as the catalyst oxidized site (O_x). It has been reported [17, 19] that the controlling step of these redox reactions is the reaction of methane on the CeO_2–ZrO_2 surface; in addition, the lattice oxygen is replenished by a significant rapid surface reaction of the reduced state CeO_2–ZrO_2 with H_2O.

The advantages of using Ni as an active metal on CeO_2 and CeO_2-ZrO_2 based supports were the high reforming reactivity. Therefore, Ni/CeO_2 and Ni/CeO_2-ZrO_2 presented much higher reactivity toward the methane steam reforming than CeO_2 and CeO_2-ZrO_2. It should be noted that the adding of ZrO_2 could stabilize the surface area of CeO_2, which meant the increasing of the thermal stability, the oxygen storage capacity, and the redox property. As the reason, the steam reforming reactivity of CeO_2-ZrO_2 was higher than CeO_2. As seen from the Table 5.6, the methane steam reforming activities of Ni/CeO_2-ZrO_2 prepared by CEAs method showed highest. The result could be

explained as CEAs method could be produced the particle with high surface area, the use of high surface area of catalyst significantly reduced the degree of deactivation by thermal sintering compared to general low surface area catalyst. The carbon formation of Ni/CeO_2-ZrO_2 prepared by CEAs method was the lowest, which meant that Ni/CeO_2-ZrO_2 prepared by this method was a good reforming catalyst in term of the high resistance toward the carbon formation compared to other method [15, 17, 19, 64].

5.6 Summary

Colloidal emulsion aphrons method has a good result in a simple, effective and reliable method to prepare Ni/CeO_2 and Ni/CeO_2-ZrO_2, leading to few nanometer particles (<10 nm), with a narrow size distribution, homogeneously dispersed over the support surface, high catalyst performance. The main advantages of the method were produced catalyst in the high surface area, controlled the particles size to a great extent, reduced the metal particles directly in the CEAs, obtained bimetallic particles at room temperature, and no effect of support on the formation of the particles.

All the synthesized catalysts were examined for methane steam reforming process. Ni/CeO_2 and Ni/CeO_2-ZrO_2 presented much higher reactivity toward the methane steam reforming than CeO_2 and CeO_2-ZrO_2. It should be noted that the adding of ZrO_2 could stabilize the surface area of CeO_2, which meant the increasing of the thermal stability, the oxygen storage capacity, and the redox property.